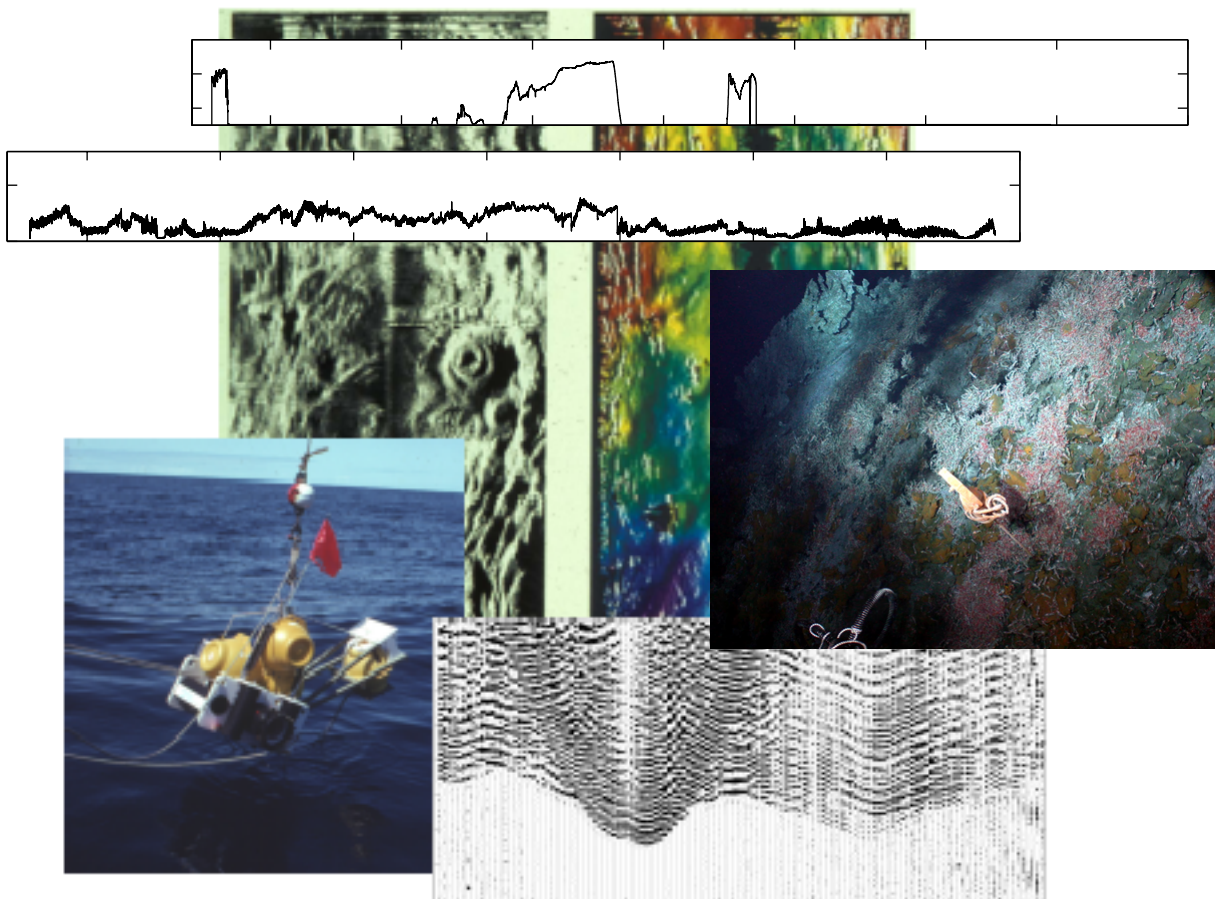


# Seismicity and Fluid Flow of the TAG Hydrothermal Mound

PIs: Robert Reves-Sohn, Susan Humphris, and J. Pablo Canales  
*Woods Hole Oceanographic Institution*

## Executive Summary



## Table of Contents

	<b>Page</b>
1. Introduction.....	3
2. Cruise Synopses.....	4
3. Preliminary Results	
3.1 Seismicity.....	5-8
3.2 Exit-fluid temperature and tidal pressure time series.....	9-14
3.3 Seismic refraction.....	14-17
3.4 SM2000 microbathymetry.....	17-20
3.5 Water column plume surveys and heat flow.....	21-23
3.6 Sampling	
3.6.1 Biological sampling.....	24
3.6.2 Geological sampling.....	24-25
3.6.3 High-temperature fluid sampling.....	25-26
3.7 Green laser engineering tests.....	26-27
4. Appendix, Cruise Participants.....	28-30

The STAG experiment is funded by the National Science Foundation, Geology and Geophysics division of Ocean Sciences (OCE-0137329), Program Manager: David Epp.

Principal Investigators: **Robert Reves-Sohn**, **Susan Humphris**, and **J. Pablo Canales** of the *Woods Hole Oceanographic Institution*

For information, please contact Robert Reves-Sohn, [rsohn@whoi.edu](mailto:rsohn@whoi.edu).

# 1. Introduction

The Seismicity and Fluid Flow of TAG experiment (STAG) is an NSF funded program focused on the hydrogeology of the TAG hydrothermal system, with an emphasis on deducing the sub-surface patterns of fluid flow. The keystone of the experiment is the simultaneous observation of seismic activity, exit-fluid temperatures, and tidal pressures at the TAG mound. These observations are complemented by an active-source seismic refraction survey designed to image the crustal architecture of the TAG segment, with the specific goal of delineating the position of any heat sources (low-velocity zones) and/or mafic material (high-velocity zones) in the region of the active mound. The TAG (Trans-Atlantic Geotraverse) hydrothermal field (26°08'N on the slow-spreading Mid-Atlantic Ridge) is one of the largest and best-studied sites of high-temperature hydrothermal activity and mineralization that has been found to date on the seafloor. The active TAG mound is a constructional sulfide feature approximately 200 m in diameter with a central chimney that reaches to an altitude of ~80 m above the surrounding volcanic seafloor.

The STAG experiment was carried out over the course of four research legs stretching from June, 2003 to November, 2004. A variety of deep-submergence and deep-sea geophysical assets were employed, including *DSRV Alvin*, *ROV Jason2*, OBSIP short-period seismometers, and the airgun array of the *R/V Maurice Ewing*. These assets provided opportunities for a variety of ancillary observations and measurements, which we attempted to maximize via leveraging of dive and ship time and multi-disciplinary collaboration with scientists with overlapping research interests. An abridged list of measurements and observations includes:

- acquisition of 9 months of seismicity data on 13 ocean bottom seismometers
- acquisition of 12 months of exit-fluid temperature data at 21 sites
- acquisition of 6 months of tidal pressure and temperature data
- acquisition of seismic refraction data on 3 lines (2 along-axis, 1 across-axis) with 23 receivers
- micro-bathymetric mapping of the TAG mound with the SM2000 on *Jason2*
- repeat water column surveys of the TAG plume
- acquisition of biological samples under controlled lighting with enzyme fixation
- repeat sampling of high-temperature exit-fluids
- acquisition of sulfide samples for geochemical and microbiological analyses
- acquisition of sediment samples for geochemical and meiofaunal analyses
- lithostratigraphic survey of the eastern valley flank wall
- engineering tests of a novel green laser system for long-range plume detection
- acquisition of underway shipboard geophysical data
- engineering tests of deep-sea compliance sensors

Preliminary results from these observations and synopses of the individual cruises are provided below.

## 2. Cruise synopses

The STAG experiment was carried out over the course of 17 months and four research legs. The timing and primary objectives of each individual leg are described below. Participant lists for each cruise are provided in Appendix A.

- 1) Leg 1, R/V Atlantis w/ DSRV Alvin, June 21 – July 8, 2003, St. Georges, Bermuda to Woods Hole, MA (Chief scientist: R. Reves-Sohn)
  - long-term deployment of 13 ocean bottom seismometers
  - long-term deployment of 21 temperature probes
  - long-term deployment of tide gauge
  - sampling of vent fauna, high-temperature exit fluids, and sulfides
  - water column plume surveying
- 2) Leg 2, R/V Maurice Ewing, October 24 – November 9, 2003, San Juan, PR to St. Georges, Bermuda (Chief scientist: J. P. Canales)
  - short-term deployment of 10 ocean bottom seismometers
  - acquisition of airgun seismic refraction data
  - acquisition of underway geophysical data
- 3) Leg 3, R/V Knorr, March 16 – April 10, 2004, Barbados to Woods Hole, MA (Chief scientist: J. P. Canales)
  - recovery of 13 long-term ocean bottom seismometers
- 4) Leg 4, R/V Knorr w/ ROV Jason2, October 25 – November 11, 2004, Woods Hole, MA to St. Georges, Bermuda (Chief scientist: R. Reves-Sohn)
  - recovery of 21 long-term temperature probes
  - recovery of long-term tide gauge
  - microbathymetric mapping of TAG mound
  - water column plume surveying
  - sampling of vent fauna, high-temperature exit fluids, sediments, and sulfides

All four of the research legs were unqualified successes. Our scientific objectives were met or exceeded in each case, as will be appreciated by examining the preliminary results section below. Note that Stephen Low Productions funded Peter Rona (Rutgers) and Adolph Seilacher (Yale) to add an *Alvin* dive to Leg 1 as part of the “Volcanoes of the Deep” IMAX film development. Push cores of the enigmatic, hexagonally shaped sediment patterns attributed in the film to *Paleodictyon* were acquired as part of this effort. Also note that 6 students from a variety of graduate and undergraduate institutions were selected (out of an applicant pool in excess of 100) to participate in the seismic refraction field program during Leg 2 as part of an education/outreach effort to provide at-sea experience for interested students.

### 3. Preliminary results

Data analysis for all of the measurement types is underway, but owing to the complex nature and large volume of the data only preliminary results are available at this time. The two noteworthy exceptions are the water column plume survey data and the microbathymetric survey data. These datasets comprised important components of graduate theses for WHOI-MIT Joint Program students Sacha Wichers (plume survey) and Chris Roman (microbathymetry survey) – both graduating in 2005 – such that they received immediate, focused attention after they were acquired.

#### 3.1 Seismicity

Thirteen ocean bottom seismometers (WHOI D2, 4-component, short period geophones) were deployed around the TAG mound to record seismicity on the TAG segment for a period of nine months stretching from June 2003 – March 2004. The seismometers were deployed in three rings of varying aperture about the TAG mound to provide hypocentral resolution at a range of length scales (Figure 1). The instruments were free-fall deployed except for the innermost ring, which was deployed via wireline with acoustic navigation to enable precise positioning of the instruments just off the active sulfide mound. The larger scale rings will be used to examine seismicity on the axial valley forming faults of the TAG segment while the innermost ring will be used to examine fluid-induced seismicity immediately beneath the active mound.

We were able to visually examine some of the inner ring instruments on the seafloor during our Alvin dive program. This represented a rare opportunity to examine the physical position and coupling of the actual seismic sensor to the seafloor, which in general is not possible during seismic experiments. A digital image of one of our seismic stations is provided in Figure 2. Our reconnaissance confirmed a fairly well-known fact amongst ocean bottom seismologists – namely that seafloor coupling is a vexing issue for seismometers that are dropped onto volcanic seafloor. The sensors are gimballed internally such that the sensor orients itself properly regardless of the orientation of the housing on the seafloor. Vertical components are therefore generally reliable, but imperfect coupling can significantly degrade the quality of horizontal components since rocking of the sensor rotates vertical motion into the horizontal components.

The 4-component instruments (3 geophone channels, 1 hydrophone channel) were sampled at 100 Hz, generating a total of ~102 GBytes of seismic data during the 9 month deployment. Parsing of this extremely large dataset is a difficult and time-consuming process, especially considering the very high levels of seismicity we have encountered. We achieved a high level of data recovery, with 12 of the 13 instruments functioning perfectly for the entire deployment. The microearthquake records are of very high quality, with excellent signal-to-noise (Figure 3). To this point we have focused on the largest scales of seismicity detected by all four of the outer ring instruments. There are in excess of 100 events per day at this largest scale, as can be seen in the histogram in Figure xx. We have made excellent progress tuning our event detection and automatic phase picking algorithms, and we have just begun the process of hypocenter estimation. We are using grid-search methods for hypocenter estimation, which is computationally expensive but which ultimately provides the most accurate uncertainty intervals.

To this point we have been working with a single event to optimize our grid-search methods. Intriguingly enough, this event appears to be located well within the mantle at a depth of more than 7 km beneath the seafloor. The unusually high seismicity rate and deep preliminary hypocenter estimate seem to indicate that the TAG segment is unusual amongst mid-ocean ridges in its seismic character. How this relates to fluid flow, and faulting in a more general sense, are issues we will be vigorously pursuing in the immediate future.

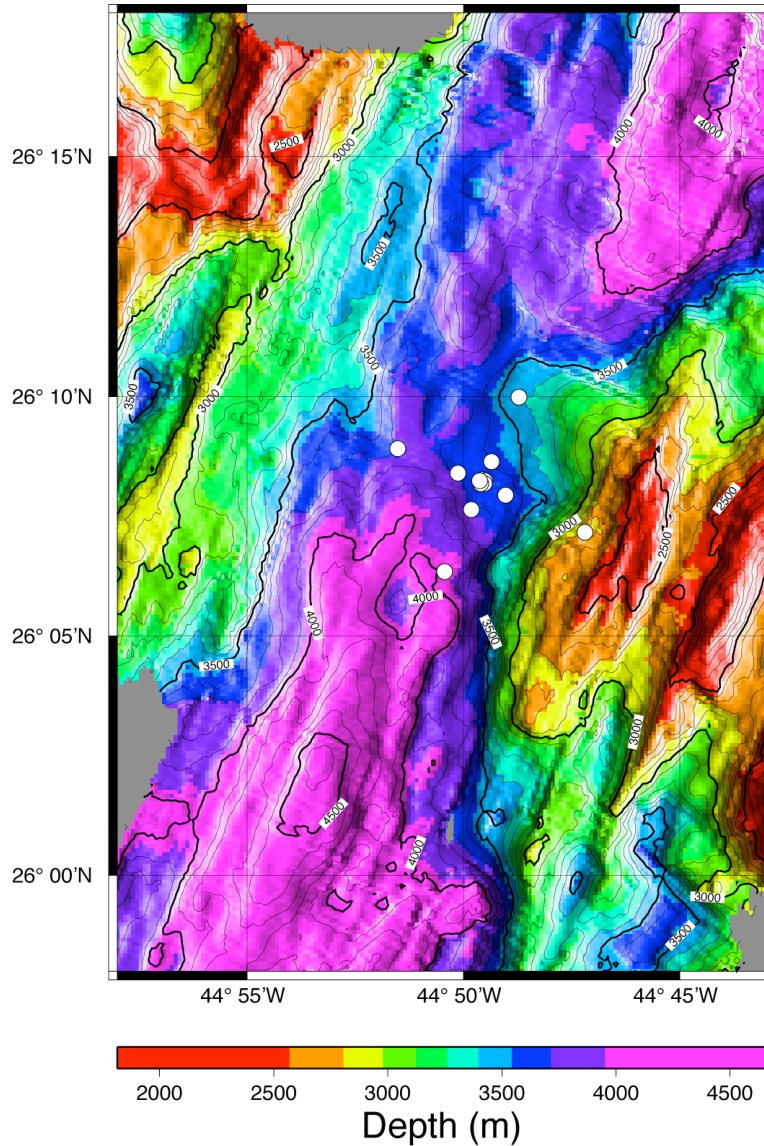


**Figure 1. Bathymetry of the TAG segment and positions of the STAG OBS network (white circles). The innermost ring of 5 OBS are clustered in this plot at the position of the active TAG mound.**

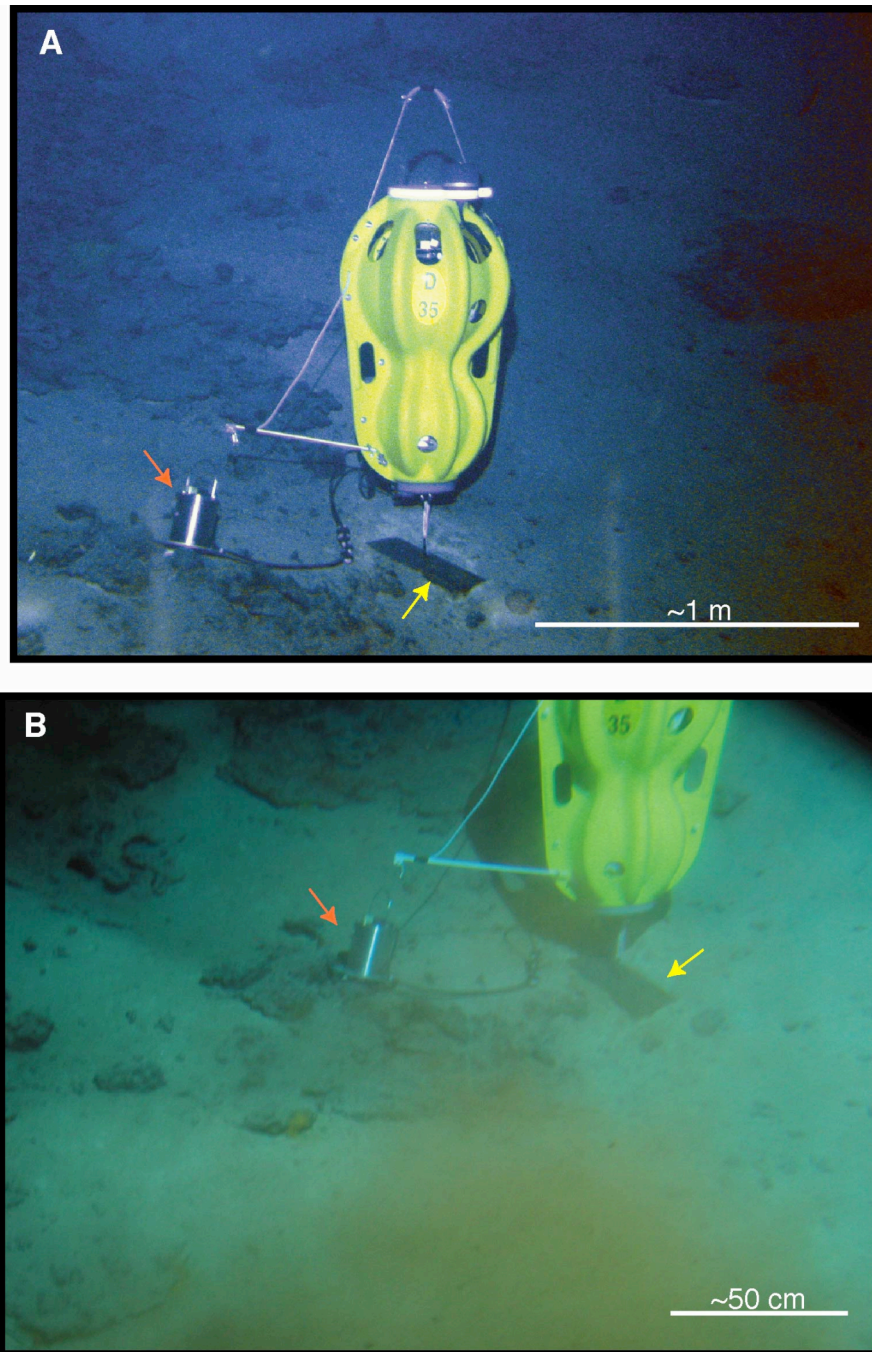


**Figure 2. Digital image (video frame grab) of inner-ring OBS from *DSRV Alvin*. OBS anchor is shown by yellow arrow, geophone sensor is shown by red arrow. The sensor is clearly perched on the side of sulfide rubble, which can be expected to affect seafloor coupling.**

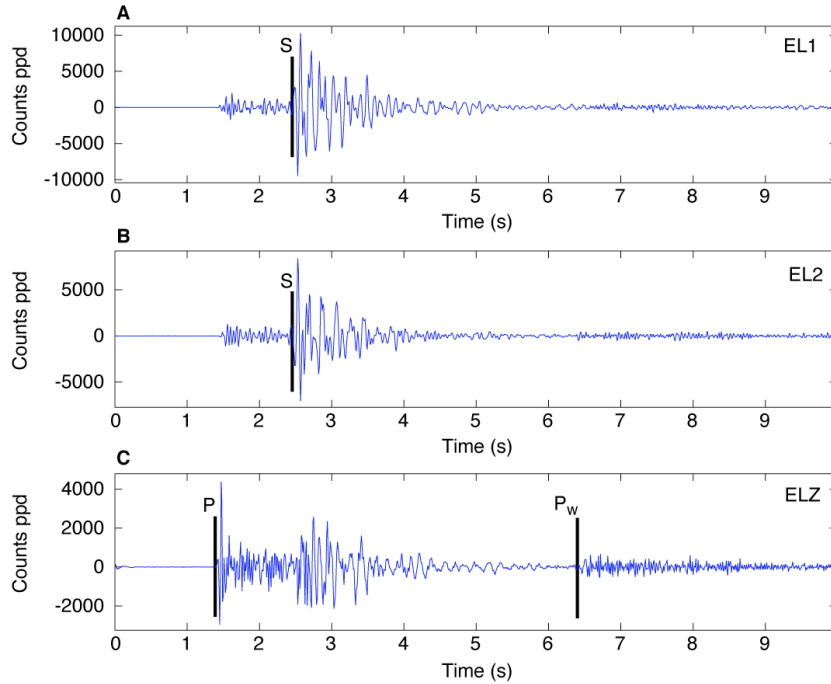


**Figure 3. Sample seismogram from a local earthquake on September 1, 2003 (0140). Horizontal (top two panels) and vertical (bottom panel) seismograms are shown with phase picks (P = direct P-wave, S = direct S-wave, P<sub>w</sub> = water surface reflected P-wave). Units are digital counts.**

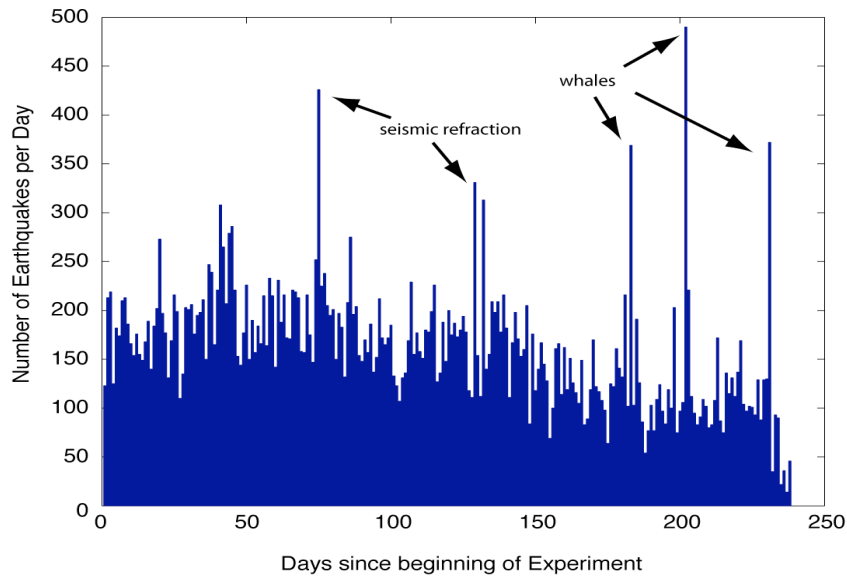


**Figure 4. Histogram of seismicity observed on all four outer ring instruments during deployment. All of the activity represents local microearthquake activity except for days 75 and 129-132, which represent seismic shooting, and days 183, 202, and 231, which represent whale calls.**

### 3.2 Exit-fluid temperature and tidal pressure time series

Two types of temperature probes were deployed on the TAG mound; (1) high-temperature (152 to 460°C) and intermediate-temperature (-2 to 124°C) probes designed by Deep Sea Power and Light (San Diego, CA) (Figure 5), and (2) low-temperature (-2 to 60 or 70°C) probes designed by VEMCO Ltd., (Nova Scotia, Canada) (Figure 6). The nature of venting at TAG is such that it is impossible to place temperature probes in the main central chimney as it is completely obscured by black smoke emanating from “blow-outs” near its base. As a result, we resorted to deploying the high- and intermediate-temperature probes primarily in these blow-outs more towards the mound perimeter in discrete regions where black smoke was emanating directly from the sulfides in the absence of chimney features (Figure 7). The low-temperature probes were placed away from the central chimney in diffusely venting cracks with shimmering water (Figure 8). Five of the seven high-temperature probes, both of the two intermediate-temperature probes, and all 12 of the low-temperature probes were recovered. High-temperature probes #1 and #7 were not found. Locations of the recovered probes on the mound are shown in Figure 9.

All of the recovered probes contained a full set of data except for low-temperature probes #3 and #10, which were apparently subjected to temperatures in excess of their tolerance and were badly burned during the deployment. High-temperature probes returned measurements every 10 minutes from 6/27/03 11:00 to 5/13/04 20:00 GMT, while the low-temperature probes returned measurements every 8 minutes from 06/27/03 11:00 to 06/24/04 19:56 GMT. Data records for the high- and intermediate-temperature probes are shown in Figure 10. Data records for the low-temperature probes are shown in Figure 11. The majority of the high-temperature probe data and ~10% of the low-temperature probe data are affected by the limited bandwidth of the data loggers. All of the probes have 8 bit A/D boards, which severely limits the effective temperature range of the measurements. Significant improvements in data quality can be obtained in the future by upgrading to 12 or 16 bit data loggers, especially for the high-temperature probes.

Stochastic analysis of the temperature time-series is being conducted by R. Reves-Sohn, with the objective of generating a stochastic hydrogeological model of sub-surface fluid flow at TAG. The basic idea is to use the statistical characteristics of the exit-fluid temperature time series’ to “condition” subsurface flow models incorporating realistic physics of flow in permeable fractures (which have now been carefully mapped at TAG with the new SM2000 data). Because temperature is a conservative tracer, analogous to the concentration of a non-reactive solute, the basic framework of stochastic hydrogeology developed for terrestrial aquifers can be directly applied to the problem. Un-clipped temperature records from the low-temperature probes are highly complex with a rich spatial correlation structure. Discrete “events” are clearly evident in the data, but there are no two probes that respond to an identical set of events. To this point we have succeeded in characterizing temperatures in diffuse flow regions with Gamma distributions, which will be an important constraint for the generation of stochastic models. Investigations to elucidate the nature and timing of the events are ongoing.

A SeaBird SBE26 Wave and Tide Gauge measured pressure and temperature at a seafloor position ~400 m northwest of the TAG mound once every 10 minutes for the first 6 months of the experiment. Tidal periods are clearly evident in power spectra of the exit-fluid temperature data (Figure 13). Intriguingly, the amplitude of the tidal oscillation in the temperature records is

often directly proportional to the instantaneous mean temperature value. This is a novel observation that will be used to constrain the mechanism by which tidal forcing modulates subsurface flow. It also underscores the importance of the Gamma distribution, in which the mean and variance are linearly related, to modeling subsurface flow. Eventually the exit-fluid temperature time-series data will be combined with the seismicity data to examine the linkages between faulting and fluid flow at TAG. This analysis is likely to focus on episodicity as a measure of correlation, but the methods ultimately used will depend on the results of the microearthquake analysis.



**Figure 5. DSPL high-temperature probe.**



**Figure 6. VEMCO Minilog-T data logger (scale bar in mm).**

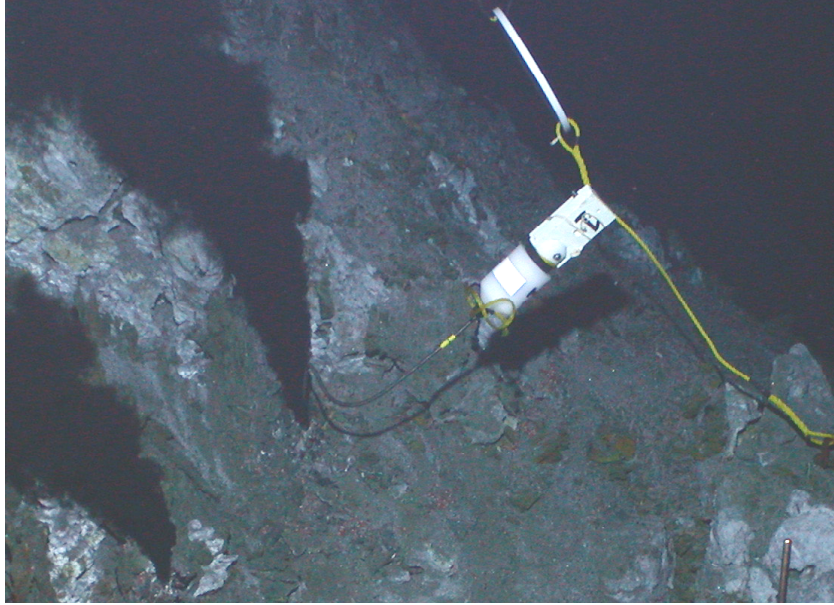


**Figure 7. Example of high-temperature probe lanced into blow-out orifice venting high-temperature fluids near bottom of central chimney complex. The tip of the probe housing the thermistors extends several inches into the orifice. A white block of syntactic foam is attached to the aft end on the data logger housing to bring the instrument package closer to neutral buoyancy. A white bucket lid marker on yellow nylon line is visible just behind the probe.**



**Figure 8. Example of low-temperature probe wand deployed in fissure venting shimmering water. The yellow wand holds two of the VEMCO probes at its base, which penetrate through the sediment veneer on the surface of the fissure. The top of the wand has a T-handle for ease of handling with *Alvin* or *Jason2* manipulators.**

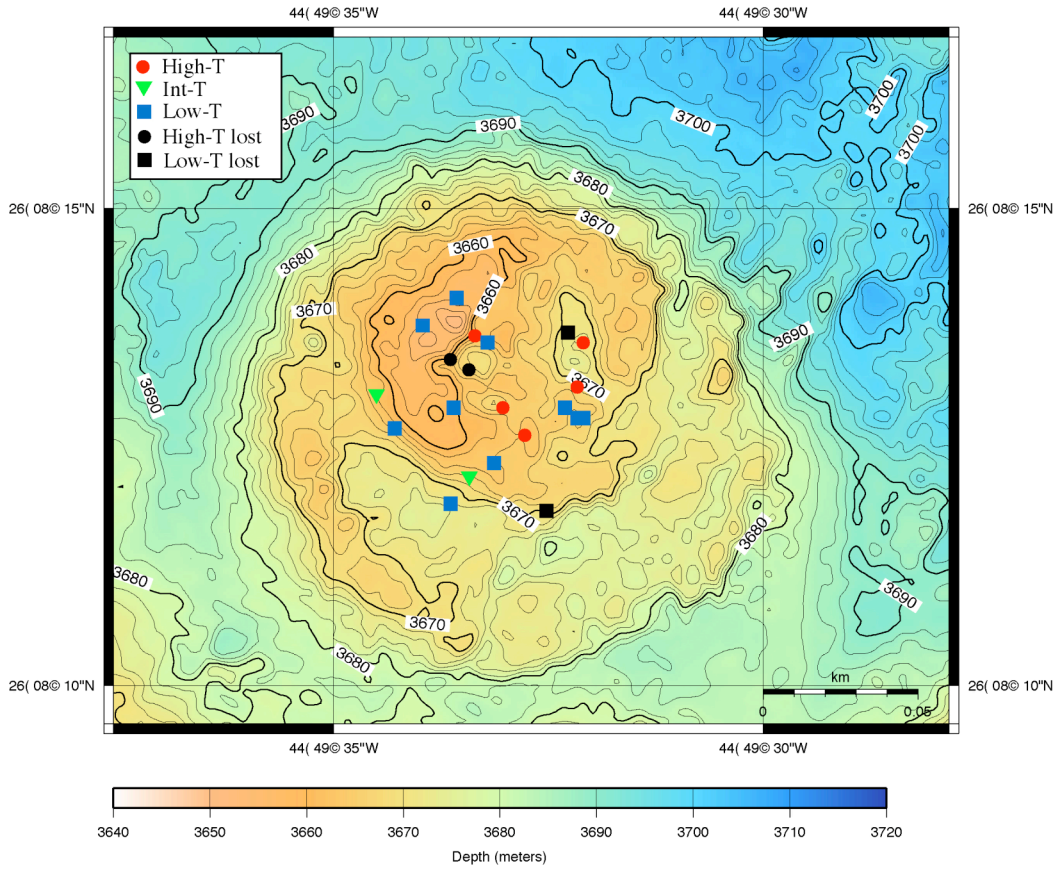


**Figure 9. TAG mound DSL-120 bathymetry with location of temperature probes.**

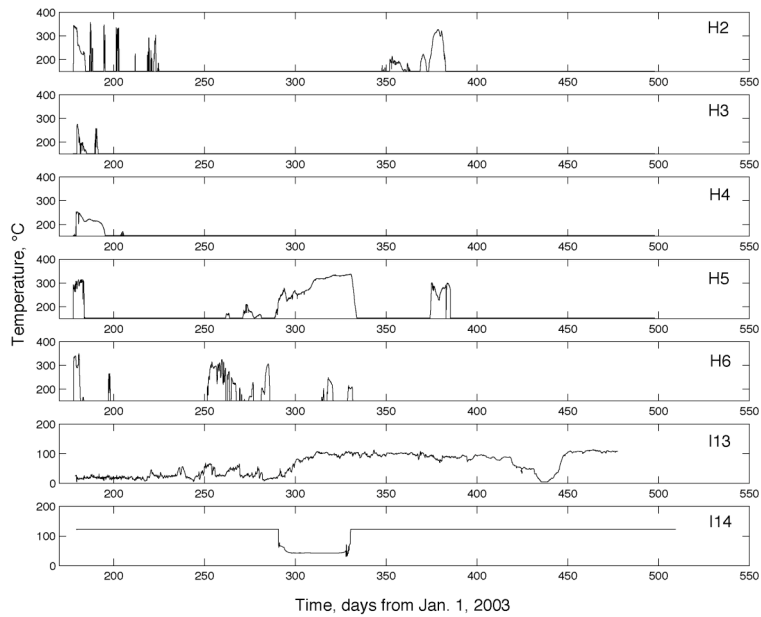


**Figure 10. High-temperature and intermediate-temperature probe data records. Note how most records clip either high or low – indicating the need for greater bandwidth in the data loggers.**

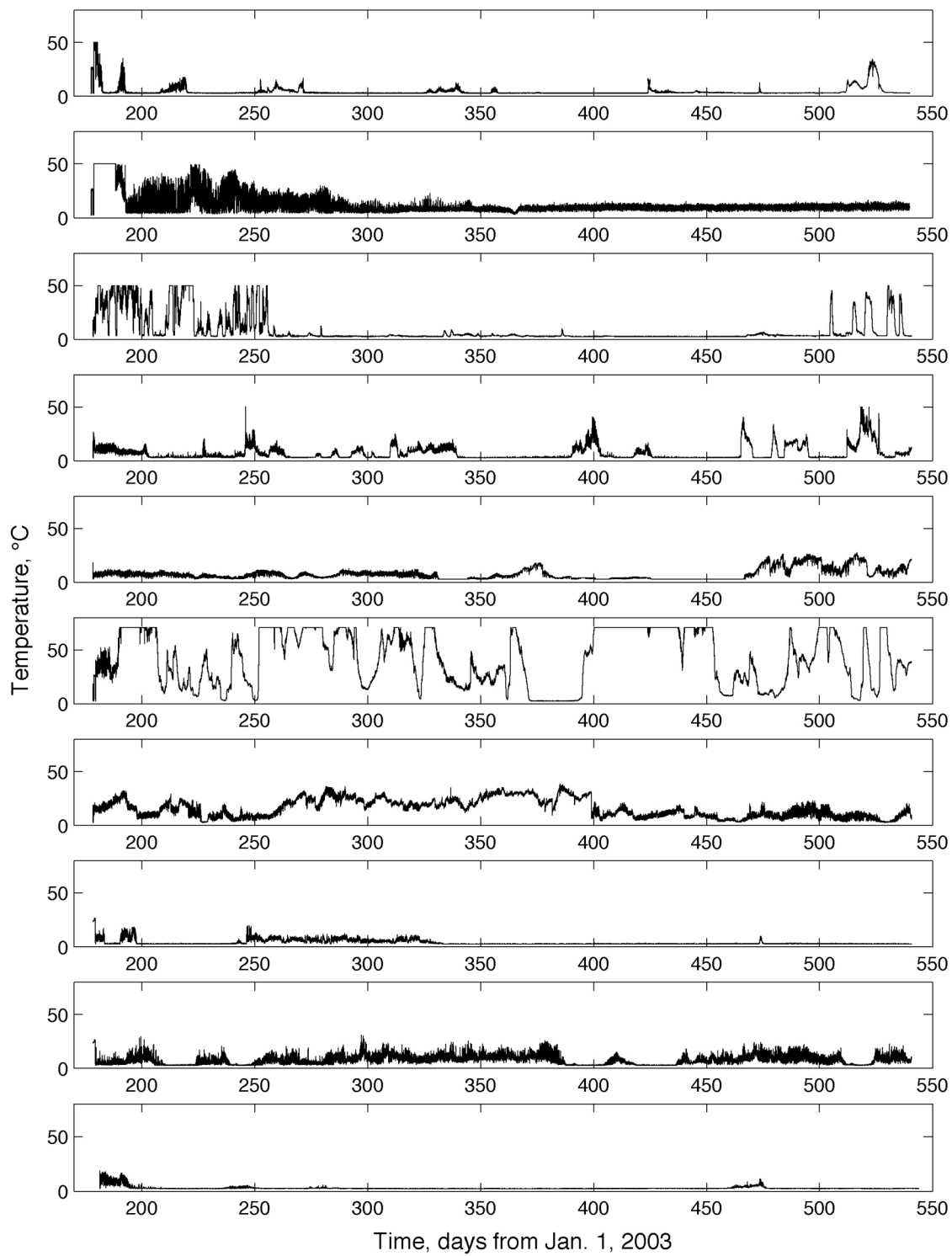


**Figure 11. Low-temperature probe data records.**

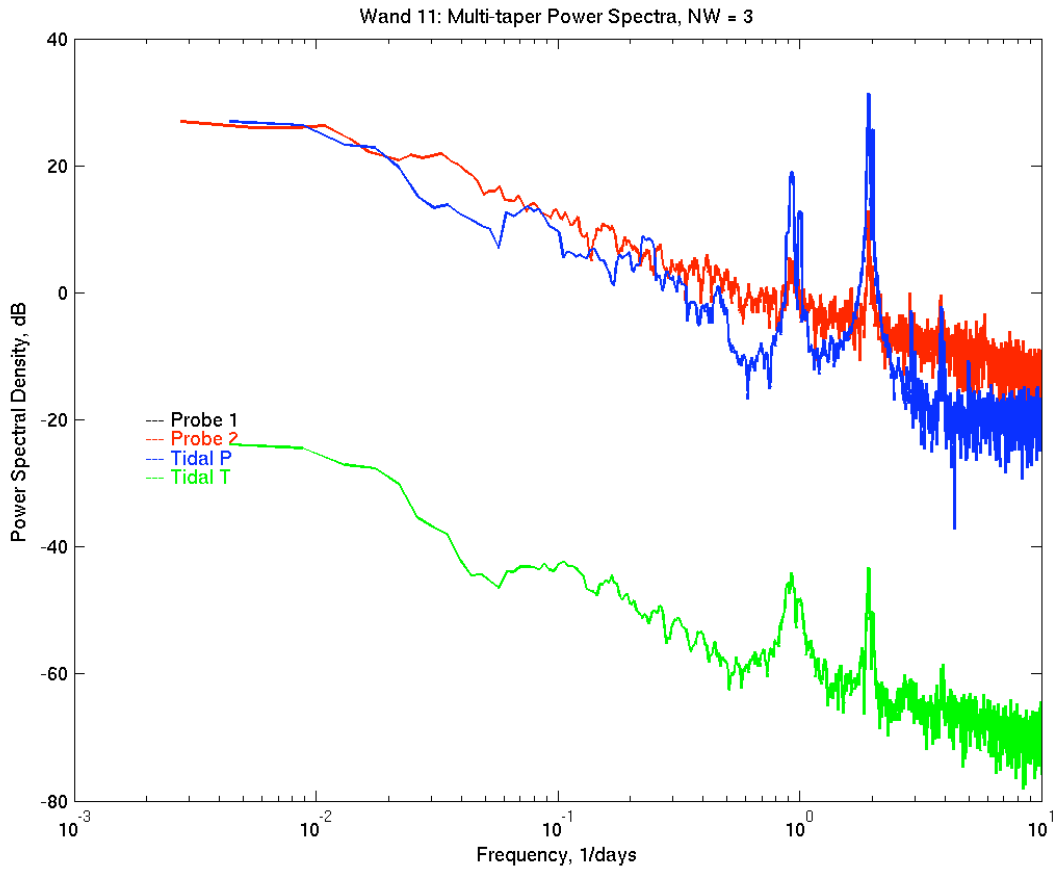


**Figure 12. Power spectra for low-temperature probe #11 (red), tide gauge pressure (blue), and tide gauge temperature (green). Note prominent spectral peaks in all records at once- and twice-a-day periods.**

### 3.3 Seismic refraction survey

One of the primary objectives of the STAG experiment is to determine the location and nature of the heat source that is driving hydrothermal convection at the TAG site. With respect to location, there are two competing models for the heat source for the TAG active mound. One model places the heat source in the neovolcanic zone, such that fluid flow pathways are provided by the axis-parallel normal faults (which may become listric at depth) associated with the eastern valley wall. The alternative model calls on discrete volcanic centers to act as the heat source for localized hydrothermal activity, and places the heat source much closer to, and essentially directly beneath the TAG active mound. With respect to the character of the heat source, there are again two competing models for the TAG system. Heat to drive hydrothermal circulation can be derived from either the extraction of latent heat of crystallization from magma chambers, or the extraction of specific heat from hot rocks across downward-migrating cracking fronts. The heat source in the former case is a discrete magma reservoir, whereas in the latter case it is a more broadly distributed zone of hot lower crust.

Both of these fundamental questions can be addressed by determining the seismic crustal structure of the TAG segment. We conducted a 6-day wide-angle seismic experiment using the *R/V Maurice Ewing's* 8760 in<sup>3</sup>, 20-gun array fired every 350 m. The wide-angle data were recorded by the long-term seismic network, as well as 10 LDEO ocean bottom seismometers that were deployed for the duration of the shooting. Our strategy was to shoot two along-axis lines and a single across-axis line passing over the top of the TAG mound (Figure 13). Eight of the ten LDEO seismometers were recovered after the first along-axis line and redeployed along the second along-axis line to provide maximal resolution with limited resources.

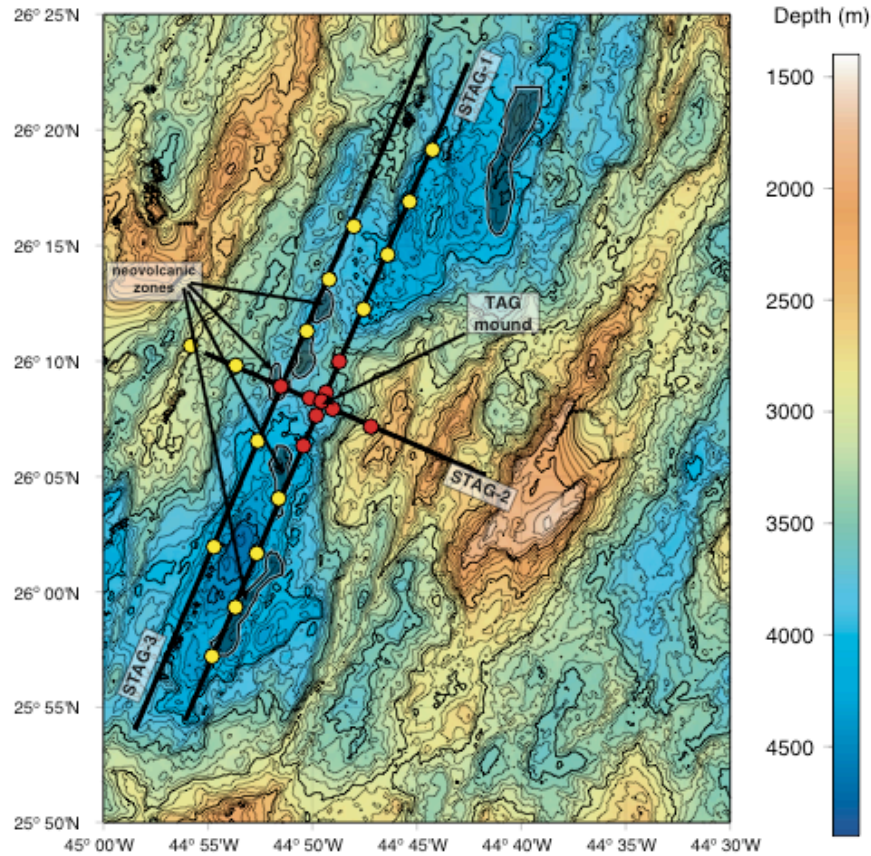


**Figure 13.** Bathymetry map of the TAG segment with seismic refraction experiment layout. Red circles mark the position of the long-term seismometers, yellow circles are short-term seismometers. Black lines are the seismic lines upon which refraction data were acquired.

Our refraction data appear to support Tivey and Schouten's assertion that the TAG mound is situated on a highly tectonized hanging wall of an active normal fault where lower crustal and/or upper mantle material is being exhumed to the seafloor. At this point it appears that TAG is the only high-temperature deep-sea vent field that has been demonstrated to NOT be underlain by a crustal reservoir of melt. These results have important implications for the hydrogeology of the TAG mound, and we will be working to integrate the refraction results into our final subsurface flow models.

Analysis of the seismic refraction data is being conducted by J. P. Canales. Compressional body-wave arrivals have been picked for all of the 2-D lines and these arrival times have been inverted against a best-fitting 1-D model to produce tomographic images of velocity perturbations along the 2-D lines. Representative record sections from individual instruments are shown in Figure 14, and our preliminary velocity models are shown in Figure 15. Resolution and sensitivity tests are ongoing, but the preliminary models clearly show that there are no pockets of volcanic heat below the TAG mound – ruling out the hypothesis that fluid flow is driven by local volcanism. To the contrary, it is evident that lower crustal and/or upper mantle material is being progressively exhumed along the eastern valley fault, which apparently extends to considerable depth into the mantle. The immediate conclusion is that the heat source driving convection at TAG is either a cracking front into the mantle or a volcanic source on the west side of the axial valley that is too deep ( $> 5$  km below seafloor) to see in our imagery – we find no evidence for low-velocity zones or partial melts anywhere along the TAG segment in our data.

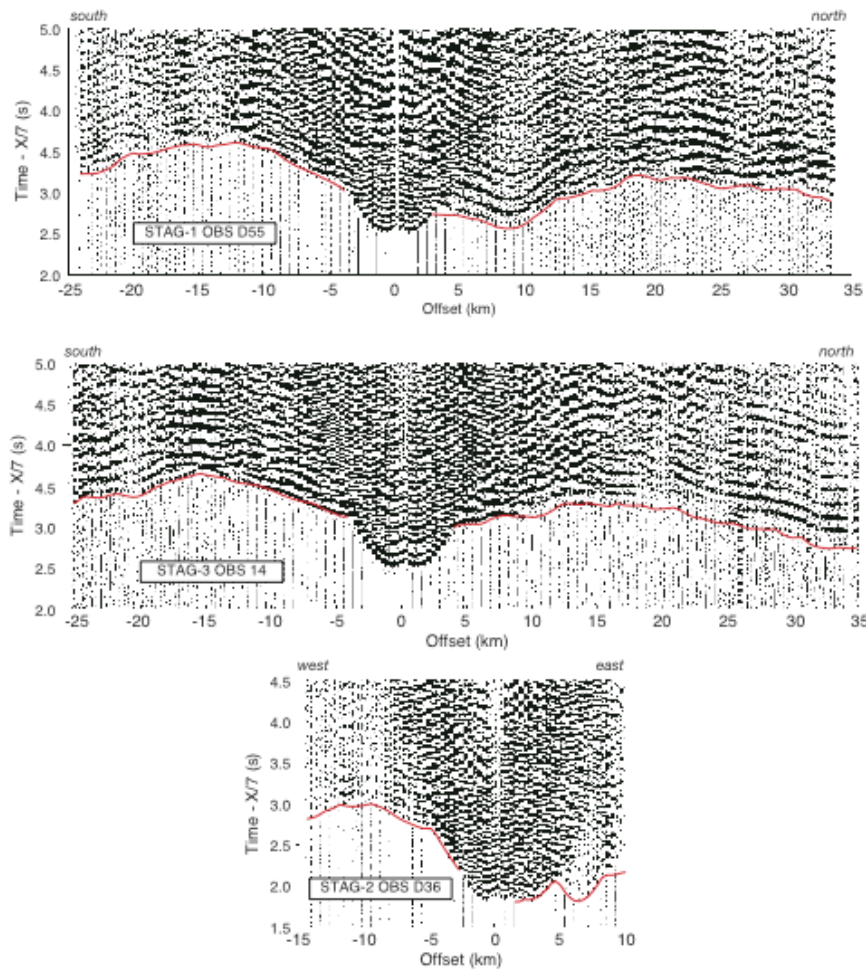


**Figure 14.** Representative record sections for seismic refraction profiles (top two are along-axis lines as referenced in Figure 13, bottom is across-axis line). Red lines are predicted travel times from preliminary models.

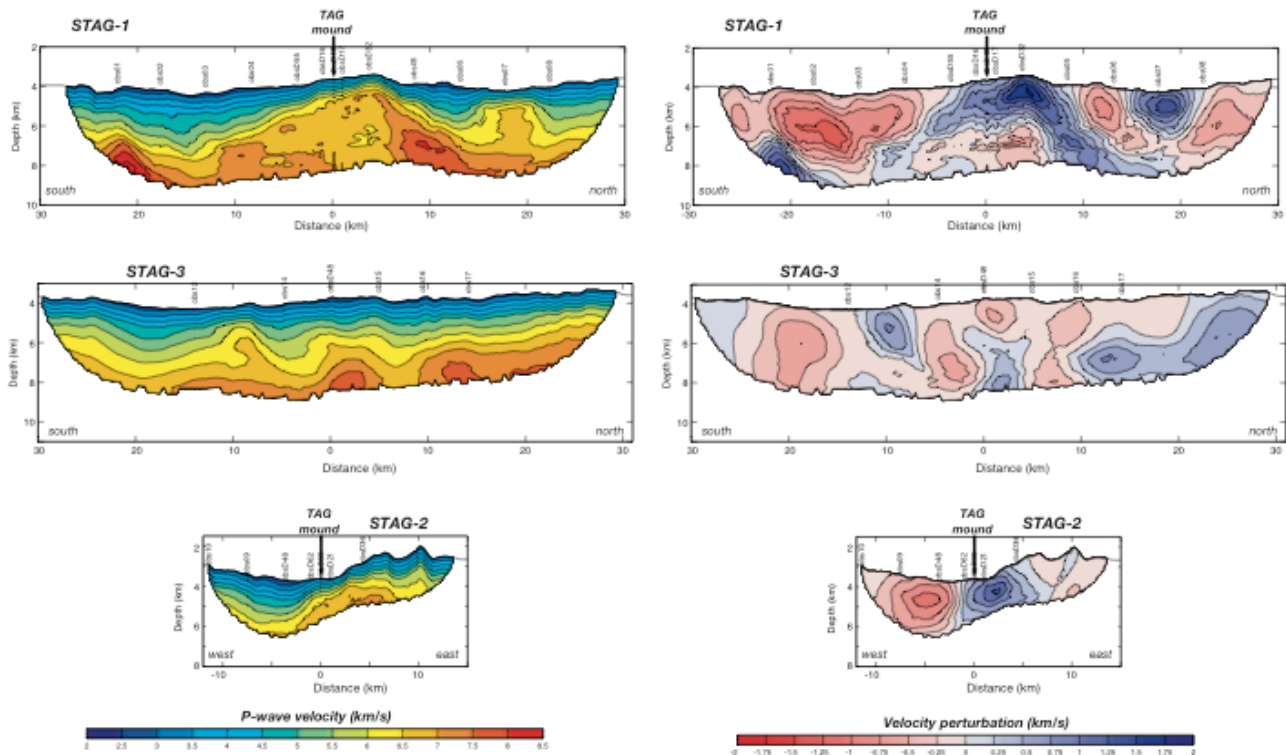


**Figure 15.** Two-dimensional travel time tomography inversions. The TAG mound is located over a large high-velocity anomaly (STAG-1), whereas crustal structure on the west side of the axial valley (STAG-3) is more typical of magmatically constructed oceanic crust. Note the asymmetric structure across the rift valley (STAG-2), indicative of large-scale faulting on the eastern valley wall.

### 3.4 SM2000 Microbathymetry Survey

The SM2000 sonar was mounted to *Jason2* to collect bathymetric data during Leg 4. Chris Roman, a WHOI-MIT Joint Program graduate student, participated in the cruise with the explicit goal of applying new techniques for optimizing the spatial resolution of microbathymetric surveys. A dense set of tracklines were selected (Figure 16) so that the majority of the mound, and high relief regions in particular, was surveyed multiple times and from a variety of azimuths. The surveys were flown with vehicle altitudes between 15 and 20 meters using the auto-altitude capability of the *Jason2* control system with a nominal forward vehicle speed of 0.5 knots.

The bathymetric map (Figure 17) was created using a new mapping making technique that enforces consistency between the mapped terrain and the ROV navigation data. Short sections of vehicle navigation are used to create small terrain maps, and these small maps are then compared and shifted to create a more consistent terrain representation in regions where they overlap. In effect, the vehicle navigation data is re-estimated to minimize bathymetric misfit in regions with significant overlap. The total terrain map is then created as a composite of all the small maps. This process minimizes errors and artifacts caused by inaccurate vehicle navigation.

The bathymetry data were imported into Fledermaus where they were rendered into a 3-D surface, allowing for perspective views of the mound from arbitrary positions, and careful mapping of the fractures that criss-cross the hanging wall in the TAG mound region. A close-up view of the mound proper is provided in Figure 18. A perspective view of the mound from the

south (Figure 19) reveals that the mound is characterized by a set of circular ridges leading to the central chimney complex that reaches an altitude of ~80 m above the local seafloor. The mound is tilted downwards to the east, most likely as a result of anhydrite dissolution in colder subsurface regions away from the present-day locus of heat flow in the northwest corner of the mound.

The resolution of this new map represents a significant improvement compared to its predecessor generated using the DSL-120 system, and is arguably one of the highest resolution maps ever generated on the deep seafloor. The two ODP re-entry cones deployed on the mound are clearly visible in the bathymetric map, providing unequivocal evidence that sub-meter lateral resolution has been achieved. Some striping remains in the imagery, which appears to be the result of timing differences between the various clocks running on Jason2. Most importantly, the high-resolution map is allowing us to develop a detailed understanding of the morphology of the TAG mound and its relationship to the complicated fracture pattern in the underlying volcanic rock. This information will significantly improve the accuracy of the hydrogeologic model being developed for TAG.

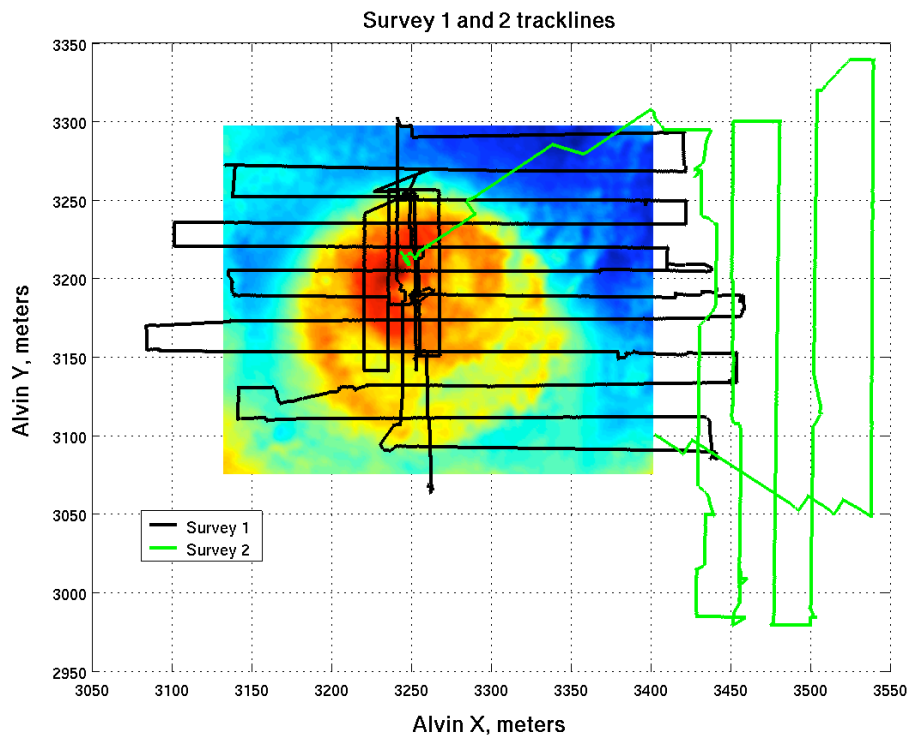
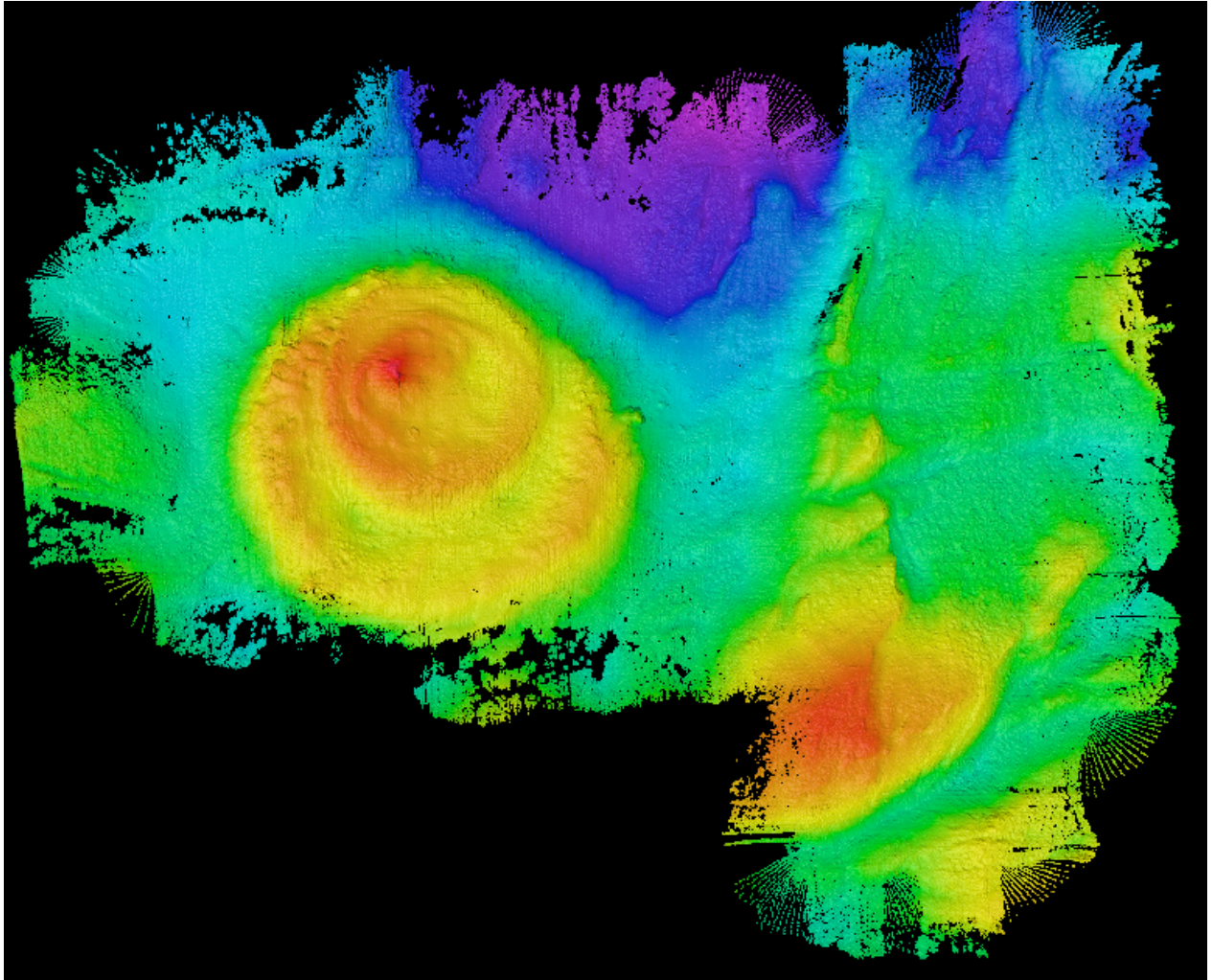
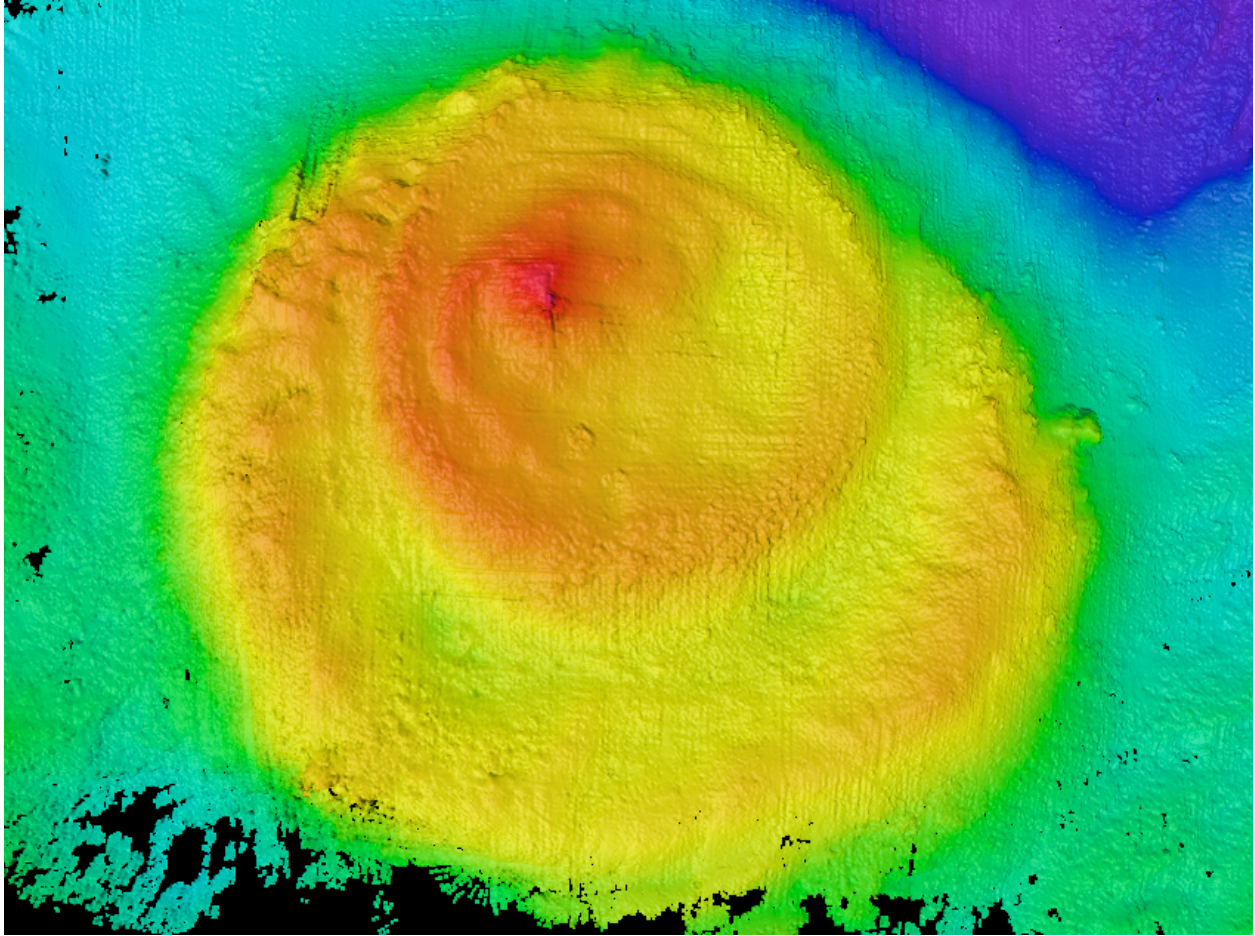


Figure 16. Survey tracklines superimposed on pre-existing DSL-120 bathymetry.



**Figure 17. New SM2000 bathymetric map of the TAG mound and environs.**



**Figure 18. Zoom-in on the TAG mound in the new bathymetric map.**

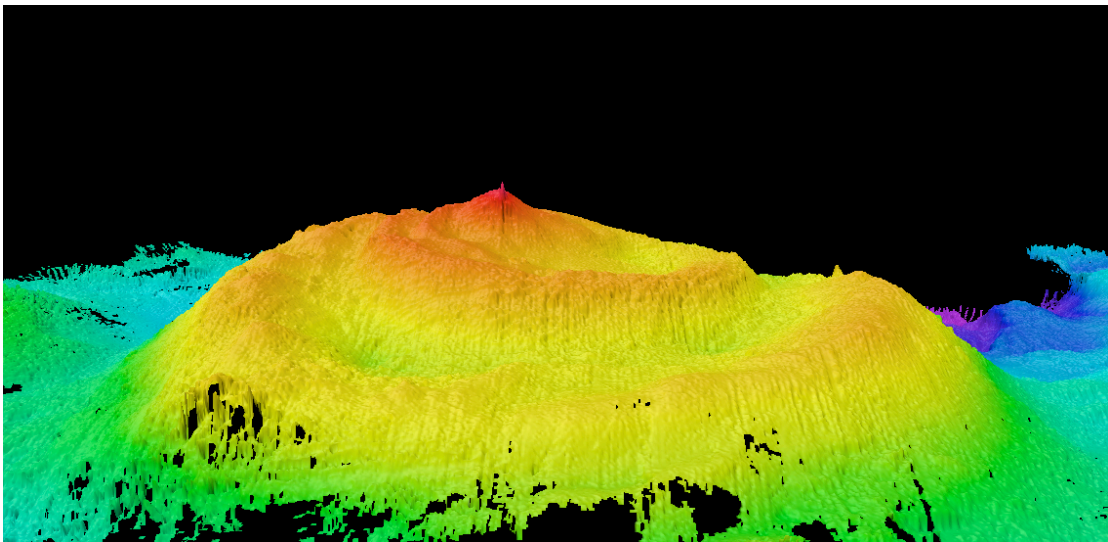


**Figure 19. Perspective view of TAG mound from south (no vertical exaggeration).**

### 3.5 Water column plume surveys and heat flow

Heat flow is one of the key first order parameters to constraining the magnitude and vigor of fluid flow at the TAG mound. Unfortunately, heat flow is a notoriously difficult measurement to make in areas of vigorous convection such as the TAG mound. At the present time the perhaps the most rigorous method for estimating aggregate heat flow is to survey the water column anomaly generated by high-temperature fluid discharge at the seafloor. If the background hydrography of the water column is known, then the rise height of the plume can be used to constrain the heat flux of the convection system.

In order to constrain heat flow at TAG we used tow-yo methods to survey the water column plume anomaly during night-ops of our Alvin dive program in 2003 (Leg 1), and during Jason2 dives in 2004 (Leg 4). Sacha Wichers, a graduate student in the WHOI-MIT Joint Program, undertook the plume survey and heat flux measurements as part of her thesis research. She combined the measurements with numerical models of advection-diffusion to estimate heat flux and to assess the reliability of the empirical results.

Tow-yo profiles of the TAG plume from tracklines shown in Figure 20 are shown in Figures 21-22. The plume is observed to stretch out  $\sim 1.5$  km along the strike of the axial valley to either side of the mound, and reaches about 600-800 m across the axial valley to both sides of the mound. These images are time aliased in that the time it takes for the tow-yo survey to traverse the entire length of the plume is greater than the tidal periods that force currents within the axial valley. We understood this problem after the initial tow-yo surveys in 2003, and we deployed an upward-looking ADCP in the axial valley (Figure 23) during the Jason2 dives in 2004. Current profiles from the ADCP reveal that the tidal forcing drives complex currents that “slosh” up and down the rise axis at both the diurnal and once a day tidal periods (Figure 24). We also find evidence that internal waves play an important role in mixing the plume with the background water mass, but we do not fully understand this phenomenon, yet.

The plume rise height in our tow-yo profiles is 400-500 m, similar to previous measurements by Speer and Rona. We used dive observations and our new bathymetric map to carefully estimate the cross-sectional area of high-temperature venting and the fluid exit velocity, which, when combined with the rise height observations yield a thermal power estimate of 6624 MW (heat flux = 2208 MW/m<sup>2</sup>) for the aggregate TAG mound. This value is on the high side of previous estimates, which have been as low as 60 MW, but it appears to be the best estimate to date in that it is based on carefully calibrated measurements and is consistent with numerical models of advection-diffusion at TAG.

We also find that the entrainment coefficient used to relate tank experiments to the field data must be on the order of 0.7 as opposed to 0.25 as has been assumed in the past. This is a significant increase that seems reasonable considering that fluids at TAG discharge from a number of discrete chimneys and fissures as opposed to a single jet as in tank experiments. These results suggest that the entrainment coefficient is a variable that must be tuned for each individual vent field.

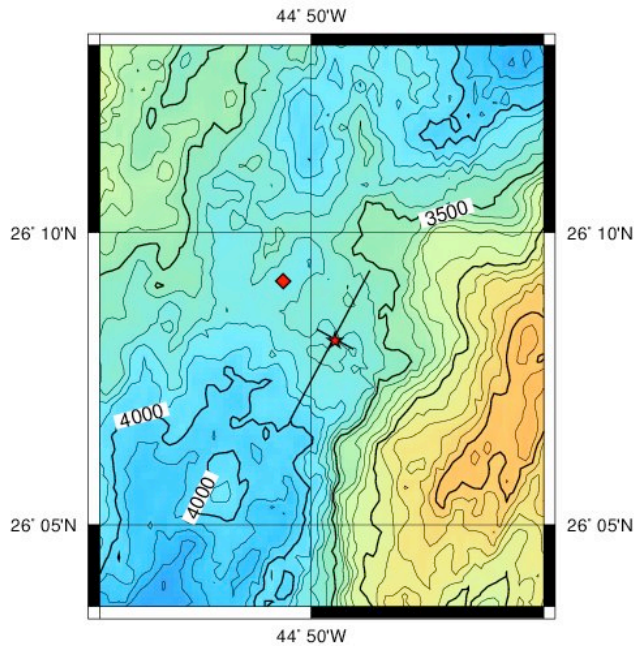


Figure 20. Tow-yo tracklines. Red square in center of valley is elevator deployment site. Red star in center of cross is TAG mound. Cross lines delineate limit of plumes in tow-yo data.

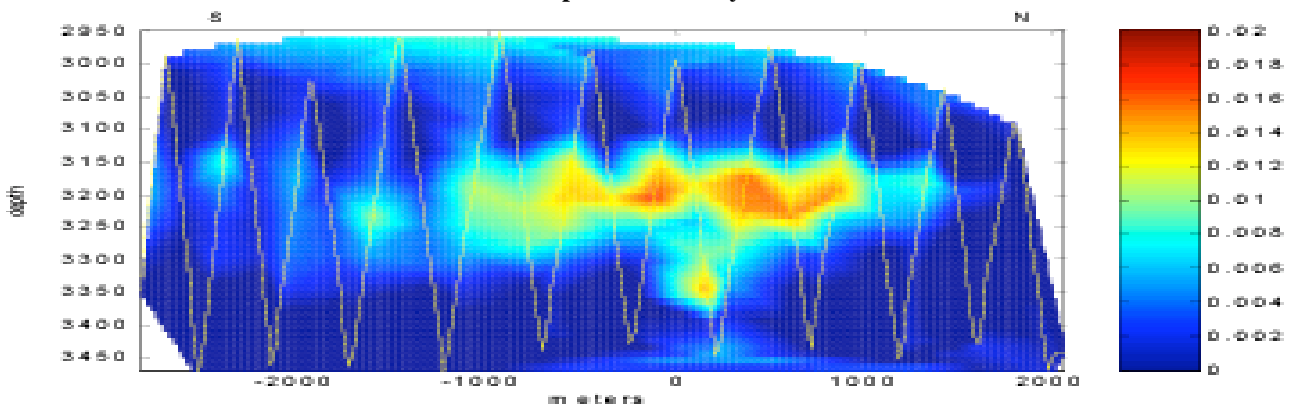


Figure 21. Along-axis tow-yo temperature anomaly profile, with TAG mound at  $x=0$  m. Tow-yo tracklines are shown in yellow.

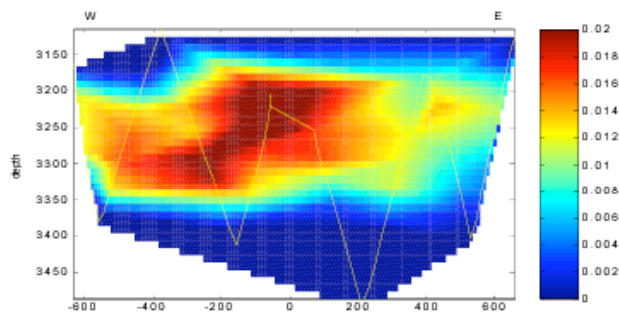


Figure 22. Across-axis tow-yo temperature anomaly profile, with TAG mound at  $x = 0$  m. Tow-yo tracklines are shown in yellow.



Figure 23. Upward-looking ADCP (far left corner of frame) mounted on Jason2 elevator during Leg 4.

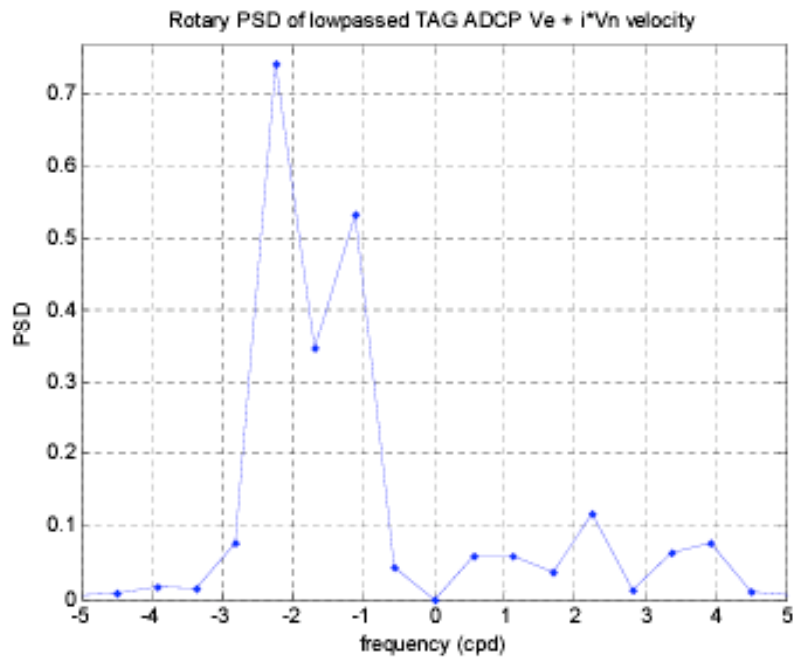


Figure 24. Rotary power spectrum from ADCP measurements. Negative values indicated counter-clockwise rotation with peaks at once- and twice-a-day periods.

### 3.6 Sampling

The Alvin dives to deploy temperature probes in 2003 and the Jason2 dives to recover them in 2004 provided the opportunity to collect geological, biological, and fluid samples from the TAG mound. We notified several groups internationally of these opportunities and then made provisions for sample acquisition in our dive plans based on the responses we received. Analysis of these samples is taking place outside the scope of our funded NSF grant, but we nevertheless

hope to incorporate the results into our broader understanding of hydrothermal processes at TAG.

### 3.6.1 Biological sampling

Biological samples were collected for Tim Shank's lab at WHOI during Leg 1 in 2003, and for Shank's lab as well as Jon Copley's lab at Southampton Oceanography Center (SOC) during Leg 4 in 2004. The primary biological objectives for the Shank lab were to collect shrimp samples for ongoing phylogenetic and population genetic studies. In addition, an instrument for fixation of deep-sea organisms at *in situ* pressure immediately following collection was utilized to conduct investigations of enzyme activity and function. Before reaching the TAG mound on the first Alvin dive in 2003, the submersible lights were extinguished save for a single light that employed a red filter. A set of shrimp samples were acquired under these controlled lighting conditions and then immediately bathed in the enzyme fixing solution so that the capability of the shrimp to "see" could be explicitly measured later in the lab.

The objectives of the SOC group were two-fold. First, shrimp were collected for histological examination to assess any seasonality in their reproductive development. Previous samples from TAG suggest aseasonal reproduction but are limited to July - September. The paucity of ovigerous females in these samples, however, could be consistent with seasonal reproduction outside this sampling period. Seasonal reproduction is now known in the bresiliid shrimp *Alvinocaris stactophila* at a cold seep, for example, with females carrying eggs from November to February/March. In addition, diagnostic morphological characters of the shrimp were measured to examine temporal variability in the population structure for later correlation with temporal variability in population genetics. Second, vent shrimp were also collected for determination of the trimethylamine oxide (TMAO) content of their muscle tissue. Deep-sea crustaceans contain elevated levels of TMAO in their tissues as an adaptation for protein stabilisation under high pressure; concentrations of this osmolyte usually increase with habitat depth. Previous work, however, shows that vent shrimp have lower levels of TMAO than expected for the depth at which they live, possibly as a result of its reduced effectiveness as a protein-folding chaperone at elevated temperatures.

Push core material was also acquired for investigations regarding the abundance and species diversity of the meiofauna (organisms between 45 $\mu$ m and 0.5mm) in chemosynthetic environments of the deep-sea (Hannah Flint, SOC), and the DNA, microbial populations, biomarkers and trace metal distribution across sharp redox boundaries associated with sulfidic sediments at TAG (Rachel Mills, SOC).

For more detailed information regarding biological samples please refer to cruise reports for the individual legs.

### 3.6.2 Geological sampling

A series of sulfide samples (e.g., Figure 25) were taken in a transect from south of the TAG mound to the black smoker complex to investigate the changes in microbiological activity with increasing distance from the area of high temperature hydrothermal discharge. Six samples were collected, ranging from sulfides almost completely weathered to Fe-oxyhydroxides, to massive pyrite showing various stages of oxidation on the lower and upper platforms, to walls of an active (366°C) black smoker chimney. Sub-samples were frozen (-80°C) for shore-based

microbiological analysis as part of the research of Dan Rogers, a WHOI-MIT Joint Program student in Marine Chemistry & Geochemistry. The remainder of the samples were dried and stored for return to WHOI where they will be available for mineralogical and geochemical analyses.

A push core of metalliferous sediment (containing iron (hydr)oxides sediments from the non-buoyant hydrothermal plume) was also acquired for analysis of transition metal uptake. The proposed project aims to investigate the link between metal uptake into colloidal plume precipitates, via adsorption and incorporation, and oceanic bioavailability of biolimiting elements (Caroline Peacock, Univ. Bristol / SOC).



**Figure 25. Sulfide sample from active chimney.**

### 3.6.3 High-temperature fluid sampling

High-temperature exit-fluid samples were acquired during both Legs 1 and 4. Chemical analyses of black smoker fluids acquired during Leg 1 will be conducted by Karen von Damm at the University of New Hampshire. Cheryl Parker, a research technician in the UNH lab, participated in the cruise to handle the fluids as they were acquired. Eight high temperature fluid samples were collected from hydrothermal vents as well as four background seawater samples. The background seawater samples were collected about 20 meters south of the TAG mound. Approximate temperature of the fluids when collected was 360°C. All samples were collected using titanium major hot water samplers. Chemical analysis will be performed for major elements and nutrients.

Analyses of fluids acquired during Leg 4 will be conducted by Darryl Green at SOC. Six high-temperature hydrothermal vent fluid samples and two background seawater samples were obtained using titanium major water samplers. Although it was not possible to obtain samples from the same orifices sampled during STAG Leg1, because one was no longer venting and the

other was covered by a flange, the high-temperature samples were collected from the main active mound in close proximity to these sources. Alkalinity, pH, [H<sub>2</sub>S], [Br<sup>-</sup>] and [SO<sub>4</sub>], were determined onboard. Further analyses will be undertaken at the Southampton Oceanography Centre, UK.

### 3.7 Green laser engineering tests

Hydrothermal plume measurements are presently made via point source measurements of thermal, particulate, or chemical parameters. Thus it is necessary to pass the sensors directly through a plume to detect it. Clearly the search for hydrothermal plumes and thus deep-sea vent fields would be facilitated if plumes could be detected from a distance. Al Bradley and Rob Reves-Sohn are PIs on a WHOI funded project to develop a green laser system capable of detecting optical anomalies in hydrothermal plumes from a distance. Clifford Pontbriant is the primary lab technician for the project, and he took part in the dive program to perform initial testing of the prototype green laser source system.

The prototype laser source system was mounted on Jason2's frame (Figure 26) and a wide-angle camera was deployed 1 m aft to provide an image of the beam outboard of the vehicle. During one of the dives, the vehicle was positioned 10-20 m away from the rising plume stem and then rotated 360° to determine if backscatter from plume particulates in the laser beam could be observed. A composite video image from this trial is shown in Figure 27.

These engineering trials demonstrated the proof-of-concept of the green laser plume detection system. We are presently seeking follow-up funding from NSF's Ocean Technology program to develop a full system for use on AUVs.

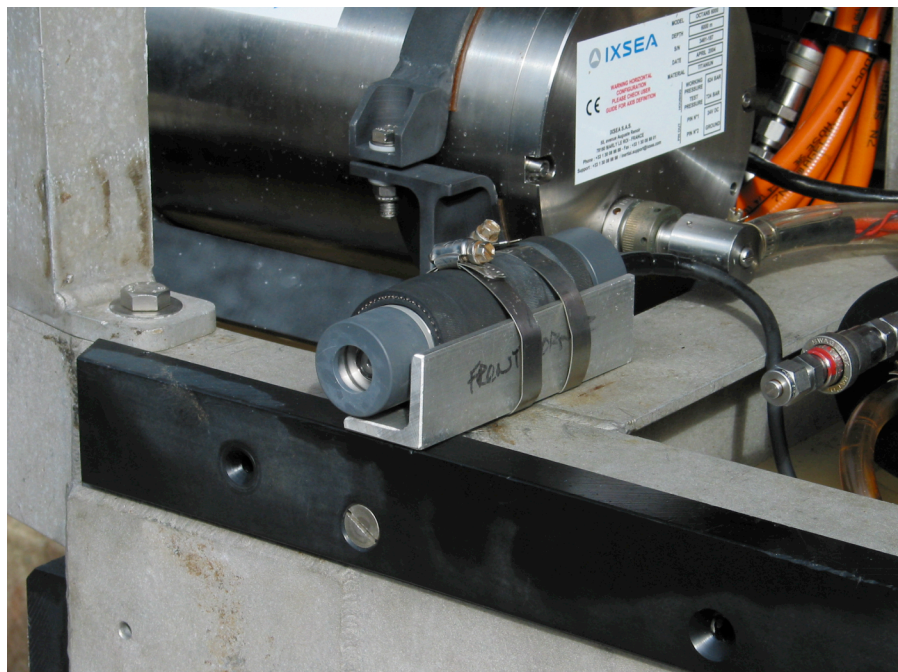
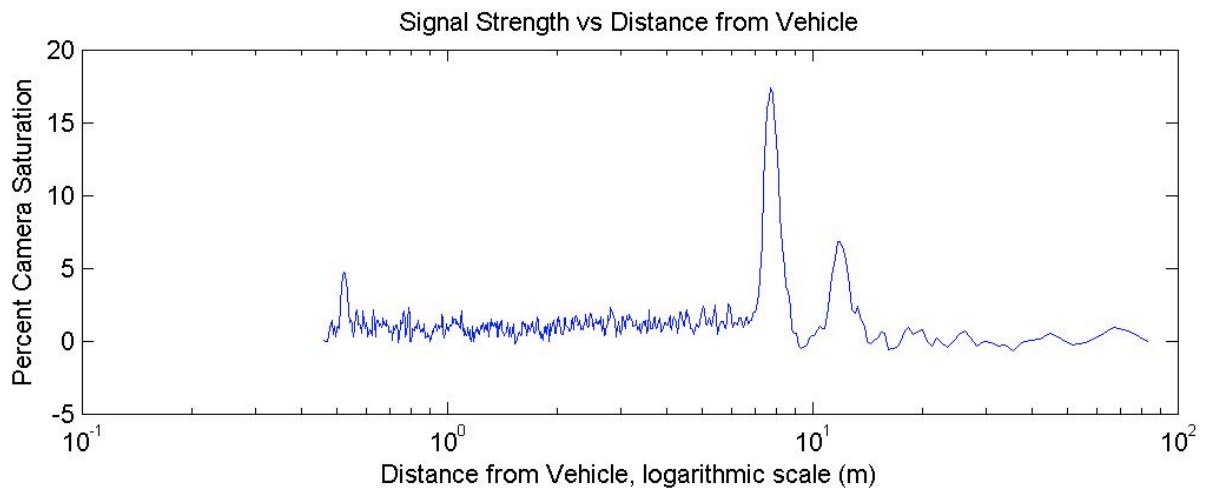


Figure 26. Green laser prototype system mounted on Jason2.

Two Second Composite Video Frame: Nov. 3, 2004, 03:39:48 GMT



**Figure 27. Backscatter results from green laser test. Top panel is a two-second composite video image of the laser beam. Bottom panel is a plot of signal backscatter strength vs. distance out-board of the vehicle.**

## **Appendix A – Cruise Participants**

Leg 1 – R/V *Atlantis* Voyage 7-36, June 21 – July 8, 2003

<b>Name</b>	<b>Position</b>	<b>Institution</b>	<b>email</b>
Rob Reves-Sohn	Chief scientist	WHOI	rsohn@whoi.edu
Susan Humphris	Co-chief scientist	WHOI	shumphris@whoi.edu
J. Pablo Canales	Co-chief scientist	WHOI	jpcanales@whoi.edu
Peter Rona	Scientist	Rutgers	rona@imcs.rutgers.edu
Adolph Seilacher	Scientist	Yale	
Steve Swift	OBS tech	WHOI	sswift@whoi.edu
Brian deMartin	Graduate student	WHOI	bjd@mit.edu
Sacha Wichers	Graduate student	WHOI	wichers@mit.edu
Diane Poehls	Graduate student	WHOI	dpoehls@whoi.edu
Cheryl Parker	Research tech	U. New Hampshire	cheryl@eos.sr.unh.edu
Francoise Labonte	Graduate student	U. Ottawa	francoiselabonte@hotmail.com
Rob Handy	OBS tech	WHOI	rhandy@whoi.edu
Victor Bender	OBS tech	WHOI	vbender@whoi.edu
Ian Rummel	Volunteer	U.S. Naval Academy	m045970@usna.edu
Dave Sims	SSSG tech	WHOI	dsims@atlantis.whoi.edu

Leg 2, R/V Maurice Ewing 03-09, October 24 – November 9, 2003.

**Scientific Party**

<b>Name</b>	<b>Position</b>	<b>Affiliation</b>	<b>E-mail</b>
J.Pablo Canales	Chief scientist	WHOI	jpcanales@whoi.edu
Rob Reves-Sohn	Co-chief scientist	WHOI	rsohn@whoi.edu
Wayne Crawford	Scientist	IPGP, France	
Spahr Webb	Scientist	LDEO	scw@ldeo.columbia.edu
Patrick Jonke	OBS Chief engineer	LDEO	pjonke@ldeo.columbia.edu
Bernard McKirieren	OBS Engineer	LDEO	bmckiern@ldeo.columbia.edu
Eric Phillips	OBS Engineer	LDEO	ericp@ldeo.columbia.edu
Janet Baran	Graduate Research Assistant	LDEO	baran@ldeo.columbia.edu
Alex Chappell	Graduate Research Assistant	U. Durham, UK	alex_chappell@hotmail.com
Andrew Delorey	Graduate Research Assistant	U. Hawaii	delorey@hawaii.edu
Katarina Jovanovic	Graduate Research Assistant	U. Houston	katarina.jovanovic@mail.uh.edu
Elena Miranda	Graduate Research Assistant	U. Wyoming	emiranda@uwyo.edu
Genevieve Parent	Under-graduate Research Assistant	Dalhousie, Canada	geparent@ggl.ulaval.ca

Leg 4 – R/V Knorr 180-1, October 25 – November 11, 2004

<b>Name</b>	<b>Position</b>	<b>Institution</b>	<b>email</b>
Rob Reves-Sohn	Chief scientist	WHOI	rsohn@whoi.edu
Susan Humphris	Co-chief	WHOI	shumphris@whoi.edu
Chris Roman	GRA	WHOI	croman@whoi.edu
Ella Atkins	Scientist	U. Maryland	ella@ssl.umd.edu
Rhian Waller	Scientist	WHOI	rwaller@whoi.edu
Clifford Pontbriand	Laser tech	WHOI	Clifford.pontbriand.03@mckenna.edu
Cathy Offinger	DSG	WHOI	coffinger@whoi.edu
Sacha Wichers	GRA	WHOI	wichers@mit.edu
Andy Bowen	DSG	WHOI	abowen@whoi.edu
Will Sellers	DSG/Exp. Leader	WHOI	wsellers@whoi.edu
Jim Varnum	DSG	WHOI	jimv@drizzle.com
Peter Collins	DSG	WHOI	pcollins@whoi.edu
Bob Waters	DSG	WHOI	rwaters@whoi.edu
Chris Taylor	DSG	WHOI	ctaylor@whoi.edu
Will Handley	DSG	WHOI	handleys@compuserve.com
Brian Bingham	DSG	WHOI	bbingham@whoi.edu
Tom Crook	DSG	WHOI	tcrook@whoi.edu
Steve Gegg	DSG	WHOI	sgegg@whoi.edu
Darryl Green	Scientist	SOC	drhg@soc.soton.ac.uk
Jon Copley	Scientist	SOC	jtc@mercury.soc.soton.ac.uk
Belinda Alker	Fluids tech	SOC	b.alker@soc.soton.ac.uk
Sarah Bennett	GRA	SOC	saroban@soc.soton.ac.uk
Caroline Peacock	GRA	U. Bristol	Caroline.Peacock@bristol.ac.uk
Carla Sands	GRA	SOC	cms600@soc.soton.ac.uk
Hannah Flint	GRA	SOC	hcf1@soc.soton.ac.uk
Magdalena Szuman	Research tech	SOC	msz@soc.soton.ac.uk